



Methodological Improvements With Conductive Materials for Volume Imaging of Neural Circuits by Electron Microscopy

Huy Bang Nguyen^{1,2,3}, Truc Quynh Thai^{1,2}, Yang Sui^{2,4}, Morio Azuma⁴, Ken Fujiwara⁴ and Nobuhiko Ohno^{1,4*}

¹Division of Neurobiology and Bioinformatics, National Institute for Physiological Sciences (NIPS), Okazaki, Japan,

²Department of Anatomy and Structural Biology, Interdisciplinary Graduate School of Medicine and Engineering, University of Yamanashi, Chuo, Japan, ³Department of Anatomy, Faculty of Medicine, University of Medicine and Pharmacy (UMP), Ho Chi Minh City, Vietnam, ⁴Department of Anatomy, Division of Histology and Cell Biology, School of Medicine, Jichi Medical University, Shimotsuke, Japan

OPEN ACCESS

Edited by:

Yoshiyuki Kubota,
National Institute for Physiological
Sciences (NIPS), Japan

Reviewed by:

Kea Joo Lee,
Korea Brain Research Institute,
South Korea
Adrian Andreas Wanner,
Princeton University, United States

*Correspondence:

Nobuhiko Ohno
oonon-ky@umin.ac.jp

Received: 04 June 2018

Accepted: 13 November 2018

Published: 23 November 2018

Citation:

Nguyen HB, Thai TQ, Sui Y, Azuma M, Fujiwara K and Ohno N (2018) Methodological Improvements With Conductive Materials for Volume Imaging of Neural Circuits by Electron Microscopy. *Front. Neural Circuits* 12:108. doi: 10.3389/fncir.2018.00108

Recent advancements in electron microscope volume imaging, such as serial imaging using scanning electron microscopy (SEM), have facilitated the acquisition of three-dimensional ultrastructural information of biological samples. These advancements help build a comprehensive understanding of the functional structures in entire organelles, cells, organs and organisms, including large-scale wiring maps of neural circuitry in various species. Advanced volume imaging of biological specimens has often been limited by artifacts and insufficient contrast, which are partly caused by problems in staining, serial sectioning and electron beam irradiation. To address these issues, methods of sample preparation have been modified and improved in order to achieve better resolution and higher signal-to-noise ratios (SNRs) in large tissue volumes. These improvements include the development of new embedding media for electron microscope imaging that have desirable physical properties such as less deformation in the electron beam and higher stability for sectioning. The optimization of embedding media involves multiple resins and filler materials including biological tissues, metallic particles and conductive carbon black. These materials alter the physical properties of the embedding media, such as conductivity, which reduces specimen charge, ameliorates damage to sections, reduces image deformation and results in better ultrastructural data. These improvements and further studies to improve electron microscope volume imaging methods provide options for better scale, quality and throughput in the three-dimensional ultrastructural analyses of biological samples. These efforts will enable a deeper understanding of neuronal circuitry and the structural foundation of basic and higher brain functions.

Keywords: scanning electron microscopy, volume imaging, charging, ketjen black, conductive resin

INTRODUCTION

The brain is composed of circuits of neurons connected to one another by neurite projections, which enables information processing in the nervous system. Impairment of neural circuitry is associated with psychiatric and neurological disorders, and a complete understanding of the wiring diagram of neuronal connections, termed the “connectome,” will provide important clues to understand brain functions and develop treatments for psychiatric and neurological disorders (Filippi et al., 2013; Deco and Kringelbach, 2014; Fornito et al., 2015). To completely understand neural circuitry, multiple imaging approaches are needed to analyze various brain structures (Le Bihan et al., 2001; Fenno et al., 2011; Grienberger and Konnerth, 2012; Lichtman et al., 2014; Ohno et al., 2016). Light microscopic technologies have enabled high-throughput and detailed analyses of neuronal circuits at a very large scale (Wilt et al., 2009; Osten and Margrie, 2013). In addition, the development of cell-specific labeling with genetically encoded tags led to marking of brain cells with different colors and tracking of specific neuronal projections at the whole-brain level (Gong et al., 2003; Livet et al., 2007). Studies on such “mesoscopic connectome” achieved big datasets and demonstrated the physical and functional connections among neurons which can span the whole brain, but a deeper understanding on neuronal circuitry has been hampered by several factors (Ohno et al., 2016). Among them, one critical factor of light microscopic approaches is the difficulty to ensure synaptic connections of fine projections, because the resolution of light microscopy is limited. The processes of neurons can be ~50 nm in diameter, and the neck of the dendritic spines can be even thinner (Briggman and Bock, 2012). These structures are too small to resolve with light microscopes for volume imaging of the brain. To overcome this problem, the standard approach is electron microscopic observation at the level of individual synapses, which unequivocally visualize fine projections and physical connections among neurons through synapses using serial section images at the ultrastructural level (Palay, 1958; Brightman and Reese, 1969). Serial electron microscope images and reconstruction of three-dimensional ultrastructural information are powerful approaches to understand the neuronal connectivity of complex brain architectures.

The three-dimensional reconstruction of biological samples has been made possible using serial ultrathin sections observed by scanning (SEM) or transmission electron microscopy (TEM; Harris et al., 2006; Bock et al., 2011; Briggman and Bock, 2012). The throughput of these microscopy techniques has recently increased significantly (Briggman and Bock, 2012). In the case of SEM, new section collection procedures such as focused ion beam SEM (FIB-SEM; Knott et al., 2008), serial block-face SEM (SBEM or SBF-SEM; Denk and Horstmann, 2004) and automated tape-collecting ultramicrotome (ATUM; Hayworth et al., 2014) are revolutionizing the field of volume electron microscopy. These new TEM- and SEM-based approaches are often complementary and differ in resolution, throughput, sample types and post-acquisition image alignment. In this context, the SEM-based methods have recently advanced

our understanding of three-dimensional structures in various organelles, cells, tissues and organisms in life science and clinical medicine, including large scale neural wiring maps of various organisms (Briggman et al., 2011; Kubota et al., 2011; Holcomb et al., 2013; Terasaki et al., 2013; Ohno et al., 2014; Ichimura et al., 2015; Kasthuri et al., 2015; Katoh et al., 2017). In addition, new devices to image large tissue areas, such as multi-beam SEM, have been developed and facilitated data acquisition from very large tissues such as whole brains (Eberle et al., 2015).

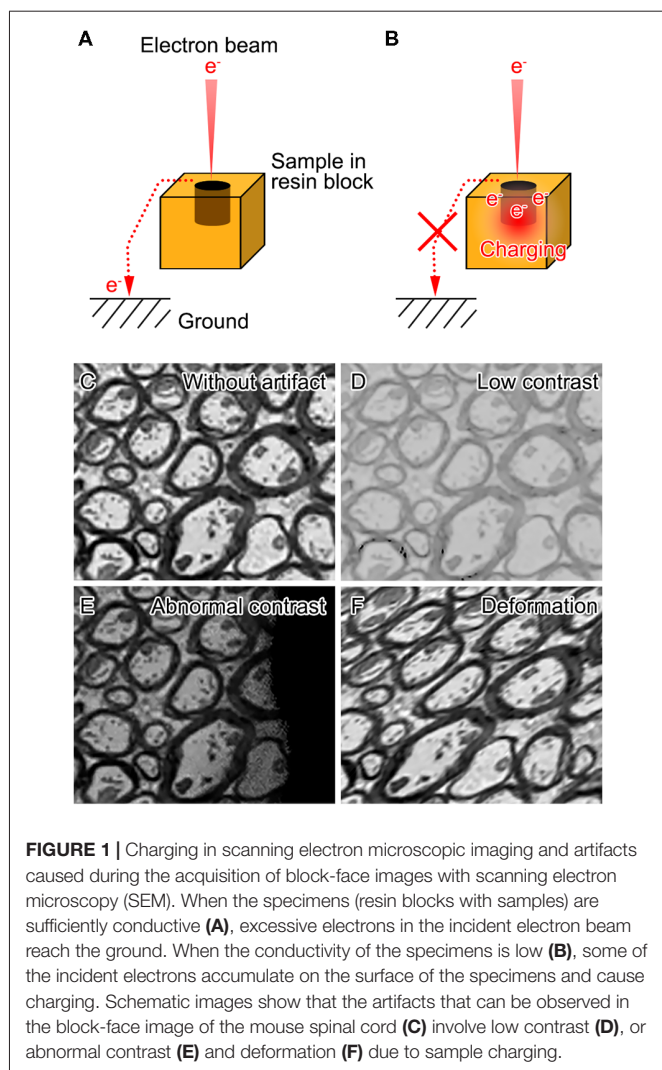
At the same time, methods using SEM for serial image acquisition generally require specific sample preparation techniques, in particular for the acquisition of large stacks of serial images with satisfactory contrast for subsequent tissue annotation, segmentation and analysis. For example in SEM imaging, the available parameter range for beam irradiation, e.g., beam current and voltage, is limited by insufficient conductivity of the biological samples. In order to acquire high contrast and high quality images, it is preferable to have sufficient deposition of heavy metals in the sample. To overcome these problems, extensive efforts have been made to improve throughput and image quality from SEM-based imaging in large tissue volumes.

Here, we review recent methodological advances in volume imaging using SEM with particular emphasis on newly developed approaches and conductive materials used in sample preparations and tissue embedding for serial sectioning and imaging, which will contribute to our understanding of the connectome in different organisms.

BASIC METHODOLOGY OF SAMPLE PREPARATIONS AND DATA ACQUISITION FOR VOLUME IMAGING USING SEM

In SEM, images are produced by focusing electron beams, scanning over the bulk specimens and detecting ultrastructural information of the specimen surface using secondary or backscattered electrons (BSE). But when BSE and/or secondary electrons derived from the flat block/section surface of resin-embedded tissue samples are detected in SEM, images which are similar to those obtained from the embedded samples in TEM can be acquired (Richards and Gwynn, 1995; Wergin et al., 1997). When low electron energies are used for the block/section face imaging with SEM, the BSE contain information only from near the surface of the embedded samples (Hennig and Denk, 2007), which can result in a depth resolution of <30 nm depending on the energy of landing electrons (Denk and Horstmann, 2004; Knott et al., 2008). For these reasons, observation of block/section faces in SEM facilitated serial image acquisition for large volume 3D reconstruction of the fine processes and synaptic connections of the nervous system, but requires specific sample preparation which can be distinct from conventional approaches for TEM or SEM observation.

Biological samples are mostly composed of light elements such as carbon, oxygen, hydrogen and nitrogen, and therefore imaging non-conductive biological specimens with SEM is often hampered by artifacts associated with charging and insufficient contrast (**Figure 1**). Various efforts have been made to achieve



higher contrast and better resolution for volume imaging of biological specimens under SEM. These efforts consist of modifications of different steps including post-fixation, staining, embedding and image acquisition (Figure 2A).

Most tissue preparation procedures for serial imaging with SEM include common fixation with chemicals such as aldehydes and *en bloc* metal staining involving osmium, uranium and lead. Following these post-fixation and staining procedures, the small pieces of tissue blocks are embedded in common resins. Efficient acquisition and analyses of serial electron microscope images are facilitated by higher contrast in cells and organelles, and therefore the procedures are designed to achieve enhanced deposition and *en bloc* staining of metals, and are now widely used to observe membranous organelles and cellular morphology (Figure 2; Deerinck et al., 2010; Tapia et al., 2012; Ohno et al., 2015; Yin et al., 2016). The *en bloc* preparation is essential for block-face imaging such as SBEM and FIB-SEM, since the block-face is imaged immediately after exposure. The *en bloc* staining is also used for imaging of the sections in ATUM or TEM because of the benefits of relatively even staining and more metal deposition for increased conductivity, which results in

improved contrast. As a consequence, lower beam doses can be used for imaging which reduces radiation damage. The methods to enhance membrane contrast used heavy metal deposition to cellular membranes (Seligman et al., 1966; Karnovsky, 1971; Walton, 1979). These methods have drawbacks, such as areas with limited staining and tissue destruction from the generation of nitrogen gas. Inhibition of nitrogen bubble formation along with staining of much wider areas was achieved in a method termed BROPA using the additional solvent and pyrogallol (Mikula and Denk, 2015). In addition, another method employed sequential modification of common preparation procedures to facilitate homogeneous metal deposition (Hua et al., 2015). These methods addressed the problems of stain penetration depth by modifying sample preparation methods for observation of large areas in brain tissues (Hua et al., 2015; Mikula and Denk, 2015). Collectively, these approaches including alternative reagents and devices which are combined with historical methods became powerful options for efficient acquisition of high quality datasets from various types of specimens including large brain tissues.

The development of improved staining procedures has been accompanied by the development of new in-chamber techniques for charge compensation that modify the acquisition condition inside of the SEM chambers. The next section introduces some of such mechanical improvements, which are termed “In-Chamber Techniques for Charge Compensation” in this review.

IN-CHAMBER TECHNIQUES FOR CHARGE COMPENSATION

Multiple approaches have been proposed which can modify the circumstances or samples in SEM chambers in order to reduce artifacts and acquire data with higher quality. For example, observation with SEM under low vacuum conditions, such as variable-pressure SEM, has often been used to acquire images from samples with problems of charging. However, these observation methods generally involve electron-gas interactions and electron beam scattering and can reduce the signal-to-noise ratio (SNR) and worsen image quality (Mathieu, 1999). To overcome the observation problems in low vacuum conditions, focal gas injection onto the block-face was used for SBEM imaging, which was termed focal charge compensation (FCC) system (Deerinck et al., 2017). This approach substantially improved charging and enabled image acquisition from samples prepared without dense heavy-metal staining. In FCC, a retractable application nozzle, mechanically coupled to the reciprocating action of the built-in ultramicrotome, was paired with a gas injection valve. The system enables the application of nitrogen gas precisely over the block-face during imaging while the high vacuum of the specimen chamber is maintained. The locally applied nitrogen gas molecules are ionized, approach the sample surface, and neutralize electrons, which charges the sample surface (Thiel et al., 1997). As a result, the FCC system does not interfere with the operation of the SBEM, but greatly reduces image artifacts in the stacks of charge-prone specimens. The addition of FCC does not affect the total time of data acquisition, but can reduce the time by allowing shorter dwelling times due to the improved SNR. Quantitatively, when

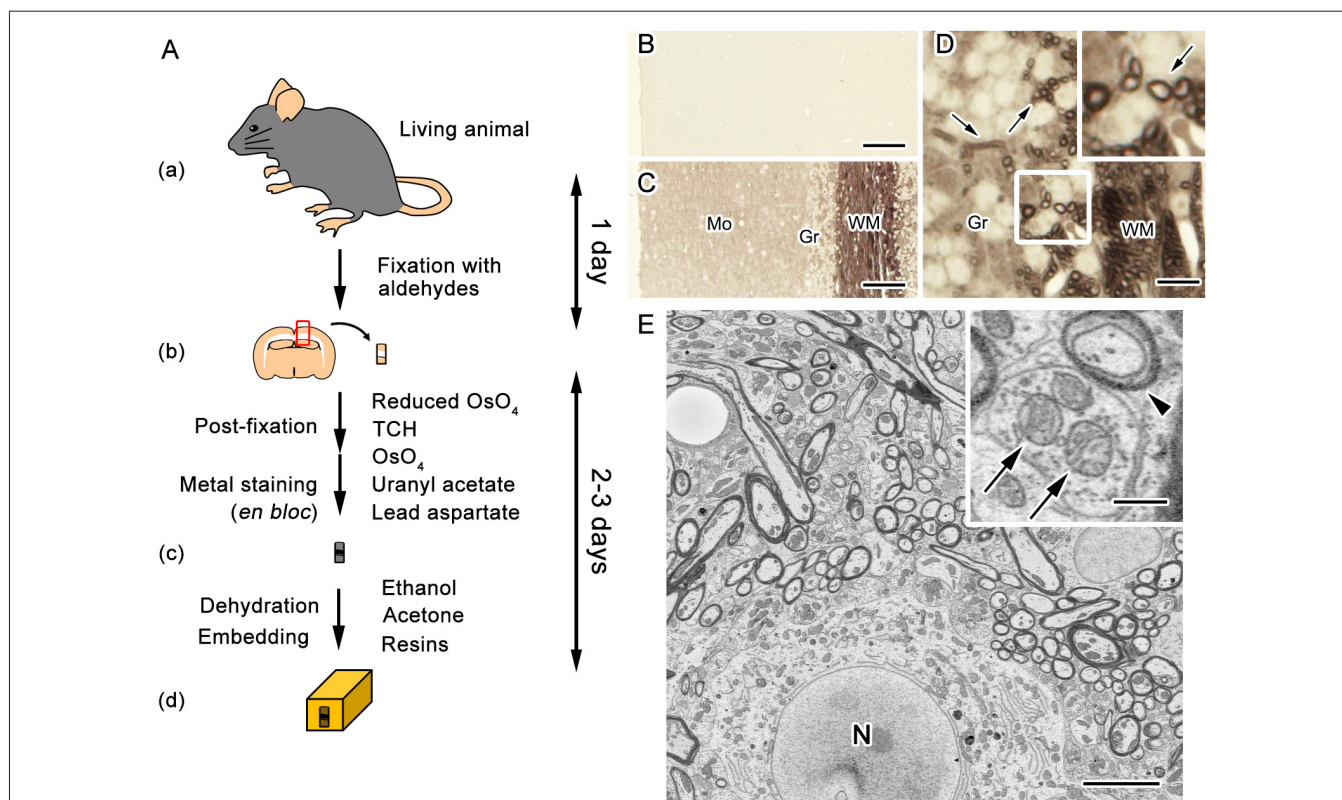


FIGURE 2 | *En bloc* staining with dense heavy metal deposition facilitates image acquisition with SEM. A diagram of the procedure for sample preparation widely used in serial block-face (SBF) imaging with SEM (A). Fixation of target tissues (mouse brain in this case) is performed by the common perfusion or immersion fixation using aldehyde fixatives (a,b). Post-fixation along with *en bloc* staining with metals is performed through treatments with ferrocyanide-reduced osmium tetroxide (OsO₄), thiocarbohydrazide (TCH), OsO₄, uranyl acetate and lead aspartate (b,c). The specimens are embedded after staining in epoxy resins following dehydration with organic solvent (c,d). Light microscope images of unstained sections obtained from cerebellar tissues embedded in epoxy resin (B–D). The sections were prepared with either the standard procedure for transmission electron microscopy (TEM) including only post-fixation with OsO₄ (B), or the procedure for volume imaging, which includes treatments with reduced OsO₄, thiocarbohydrazide, OsO₄, uranyl acetate and lead aspartate (C,D). Compared with the standard procedure for TEM (B), the procedure for volume imaging clearly visualized histological features (C), such as myelinated nerve fibers (D, arrows). Mo, molecular layer; Gr, granular layer; WM, white matter. For SEM imaging, cellular structures, such as myelin membranes (E, arrowhead) and mitochondria (E, arrows), were clearly observed in samples with dense heavy metal staining. N, nucleus. Bars: 50 μm (B,C), 12.5 μm (D), 5 μm (E) or 500 nm (E, inset). Images were adapted from Ohno et al. (2015) with permission.

increasing the accelerating voltage from 2.5 keV to 4.0 keV (60%) and increasing the pixel dwell time from 1 μs to 4 μs (4×), SNR was 28% lower using variable pressure-SEM than FCC, and the resolution obtainable by FCC was nearly the same as measured using high vacuum (Deerinck et al., 2017). Taken together, FCC is a promising approach to observe charging-prone samples by modifying SBEM system but not samples themselves.

In addition to alterations of the sample atmosphere, beam deceleration can significantly improve the contrast and resolution of images in block-face imaging of biological samples in SEM under low landing energy levels and a low beam current (Ohta et al., 2012; Titze and Denk, 2013). In the beam deceleration approach, the specimens are held at a negative bias voltage, and the electrons leaving the column are decelerated before reaching the specimens. The beam deceleration system has multiple advantages including improved detection of signals from negatively biased specimens and better resolution by very low landing energy of the incident electrons. Although the

sample conductivity is critical for the beneficial effects of beam deceleration, imaging of such conductive samples at high spatial resolution could be significantly facilitated by applying beam deceleration upon imaging in SEM.

Treatments to increase the surface conductivity of samples have been widely used in observation of biological specimens in SEM. Attempts to apply this concept to the SBEM imaging have been made in SEM chambers by automated block-face metal coating, and charging could be significantly improved during SBEM imaging (Titze and Denk, 2013). In this study, the surface of the imaged blocks was covered with thin (1–2 nm) metallic films composed of chromium or palladium using an electron beam evaporator that is integrated into the microscope chamber. In this system, the conductivity of the surface was increased by the thin metallic films prior to each cycle of imaging. The reduction in SNR caused by the metallic film is smaller than that caused by the widely used low-vacuum method. So the film coating results in better signal than the low-vacuum method, but still fully compensates any charging artifacts. In addition, one big

advantage of this in-chamber coating method is that it allows detection of secondary electrons, which in turn enables much higher acquisition speeds than BSE-based imaging. The sample whose surface was 12 mm across could be coated and imaged without charging effects at beam currents of 25 nA, and more than 1,000 serial images could be acquired under the automated cut/coat/image cycles. However, one critical drawback of this approach is the requirements for the specific devices which enable in-chamber coating of the samples with the metallic films.

Another method using plasma etching prior to imaging has been used to remove contaminants and enhance contrast in serial image acquisition using ATUM (Morgan et al., 2016). Plasma cleaning has been used to remove contaminants, and this would be helpful in ATUM since it is possible that various contaminants which perturb image acquisition can be attached on the surface of sections during sectioning, mounting on the tape and subsequent preparation for imaging. In addition, plasma etching can be used to enhance contrast in SEM imaging using secondary electrons, presumably due to the removal of specimen components near the specimen surfaces and generation of surface unflatness (Hukui, 1996). The plasma etching could be beneficial in serial image acquisition in SEM when the secondary electrons are used for imaging of the block/section faces.

The modifications of physical properties, such as sample conductivity, and improvements in observation methods have improved image quality. Dense deposition of heavy metals on specimens is beneficial for SEM imaging because it increases conductivity and improves the SNR of samples. Increasing the conductivity of the embedding media in addition to specimen conductivity could be beneficial for the observation of non-conductive biological materials. Different materials and methods for specimen embedding have improved in the life sciences and clinical medicine, and in the next section we discuss several recent studies that modified embedding procedures and media in order to facilitate serial image acquisition using SEM.

IMPROVEMENT OF EMBEDDING METHODS FOR CHARGING COMPENSATION

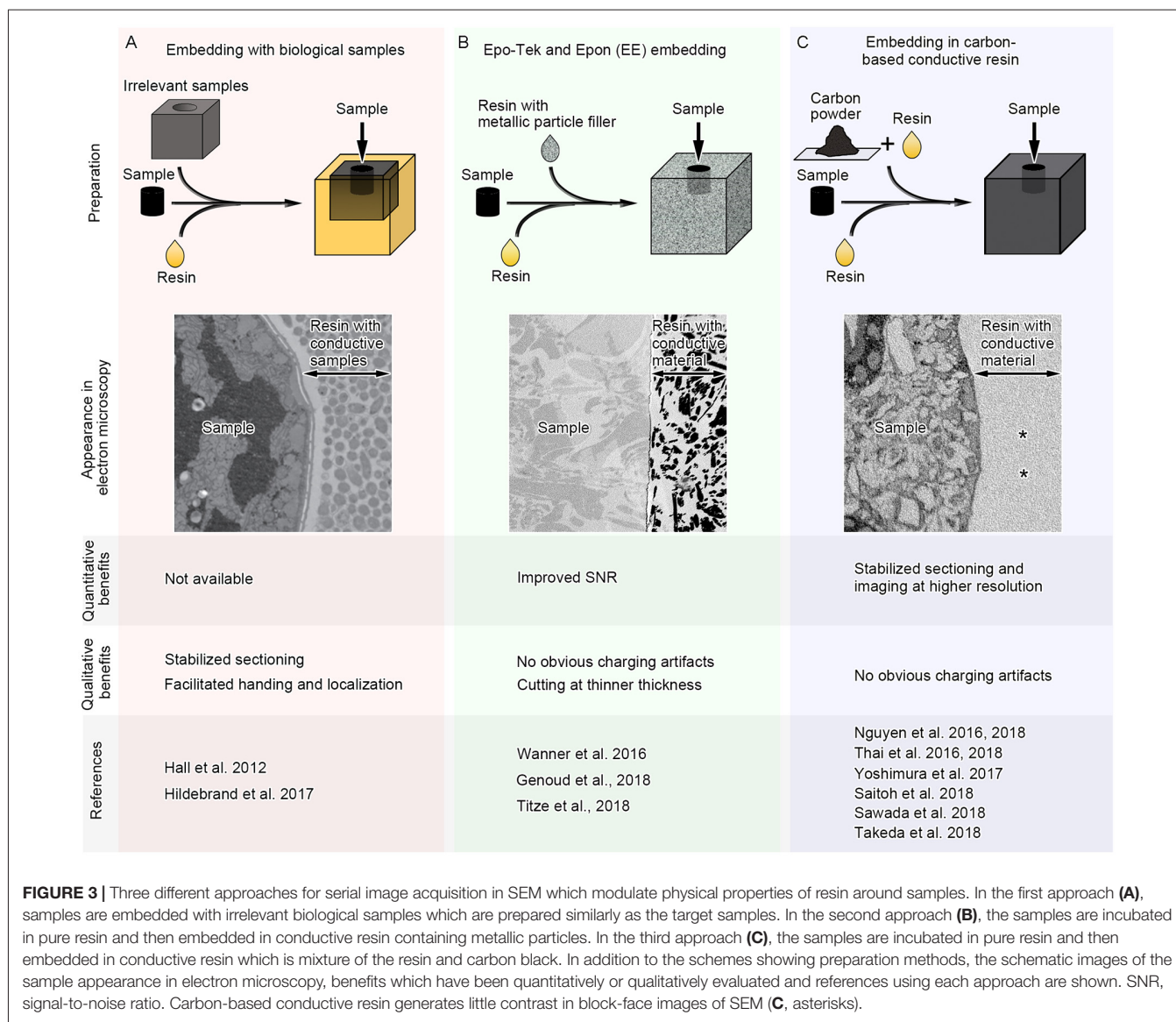
Developing new embedding media for electron microscope imaging requires consideration of the physical properties associated with the imaging procedures, such as stability in sectioning and the degree of deformation under electron beam irradiation. Sectioning with a diamond knife requires careful consideration of the physical properties of the target materials, which significantly affect knife lifetimes (Hashimoto et al., 2016). Imaging and cutting conditions, such as sample temperature, cutting speed, cutting thickness and size, knife shape and knife temperature, also affects knife lifetimes, but material hardness is the most important factor for image quality. In addition, electron beam irradiation causes thermal damage to the resin, and artifacts occur from resin shrinkage and deformation, which can be ameliorated by cooling the

samples to cryotemperatures (Luther, 2006). These artifacts also depend on electron beam properties, such as acceleration voltage strength and electron current, which can be evaluated with sections mounted on conductive tapes (Kubota et al., 2018). However, damage and structural deformation of the resin-embedded samples from electron beam irradiation may also be affected by the properties of the stained and embedded tissues.

Historically, various resins have been used for electron microscope observation of biological specimens. Early resins, such as methacrylates, developed for ultrathin sectioning and epoxy resins developed later resulted in less structural changes (e.g., shrinkage) upon curing and high stability during ultrathin sectioning and electron beam irradiation (Glauert and Glauert, 1958; Luft, 1961). Different types of resins, including water soluble and hydrophilic resins, have been developed and used for electron microscope observation, and these resins have unique properties which are suitable for different target samples and staining and observation methods (Staeubli, 1963; Leduc and Bernhard, 1967). The artifacts from shrinkage and deformation typically include depth-direction and planar shrinkage during electron beam irradiation. This type of shrinkage is obvious during SBEM imaging, when there is local failure of physical slicing in areas with intensive irradiation of the electron beam for focusing. TEM-based evaluation revealed that the stability against electron beam artifacts varies among different resins (Kizilyaprak et al., 2015). Interestingly, maximal resistance against electron beam damage is achieved by a mixture of different resins, but the exact mechanisms of improved resistance remain unclear. These studies provide options for the optimization of embedding media, which enables better stability for the imaging of biological specimens with intensive beam irradiation.

Generally, resins used for electron microscope observation have distinct physical properties compared with adjacent embedded biological specimens. Most resins are composed of light elements, which have lower conductivity than that of the embedded specimens, particularly when the specimens are densely stained with heavy metals. In addition, the hardness of the resin is altered in regions with biological specimens. These problems could be potentially solved by modifying the undesired physical properties of the resins around the samples. “Fillers” have long been used to modify the physical properties of base materials (e.g., plastics, concrete), such as electrical conductivity and hardness. It is therefore possible that those conventional or new filler materials have beneficial effects on physical properties of the resins and facilitate serial image acquisition in SEM by reducing artifacts. Recent studies have started exploring this possibility and found some promising results using different types of “fillers” beneficial for the serial image acquisition in SEM (Figure 3).

To facilitate SEM imaging, biological specimens that are not related to the experiment are embedded with the target samples. These biological specimens are used as a kind of “filler material,” which modifies the physical properties of



the surrounding resin. Biological filler materials are stained and prepared similarly to the target tissues, and therefore the physical properties of the filler and target tissues are similar. One example of the biological filler materials is tissue from the mouse brain, which was embedded with larval zebrafish for serial sectioning by ATUM (Figure 3A; Hildebrand et al., 2017). Homogenous hardness and stability of sample blocks facilitate repeated serial sectioning by ATUM and prevent heterogeneous shrinkage, deformation and folding of sections. Small larval zebrafish samples were post-fixed, stained *en bloc*, embedded into resin blocks, and finally surrounded by mouse brain tissues for stabilization during sectioning. In this study, 17,963 sections at 60 nm thickness were acquired in ATUM for serial image acquisition. In total, 244 (1.34%) sections were lost and 283 (1.55%) were partially lost, while no two adjacent sections were lost. Although more quantitative analyses on physical properties of the brain “filler materials” are

required, it is possible that filler biological samples treated and embedded similarly to the target specimens substantially improve production of and imaging from serial ultrathin sections.

Aggregated unicellular organisms can also be used as biological support materials. *C. elegans* was embedded with *E. coli* or yeast cells during cryofixation to facilitate handling and localization of the samples (Figure 3A; Möller-Reichert et al., 2003; Hall et al., 2012). The samples were still surrounded by biological material during the subsequent tissue preparation procedures, including freeze-substitution, and the resins surrounding the *C. elegans* sample at the time of observation were filled with biological material that was stained and embedded at the same time (Hall et al., 2012). Because the sample has biological components enriched with metal deposition, the regions occupied by the organism had different physical properties from bare resin.

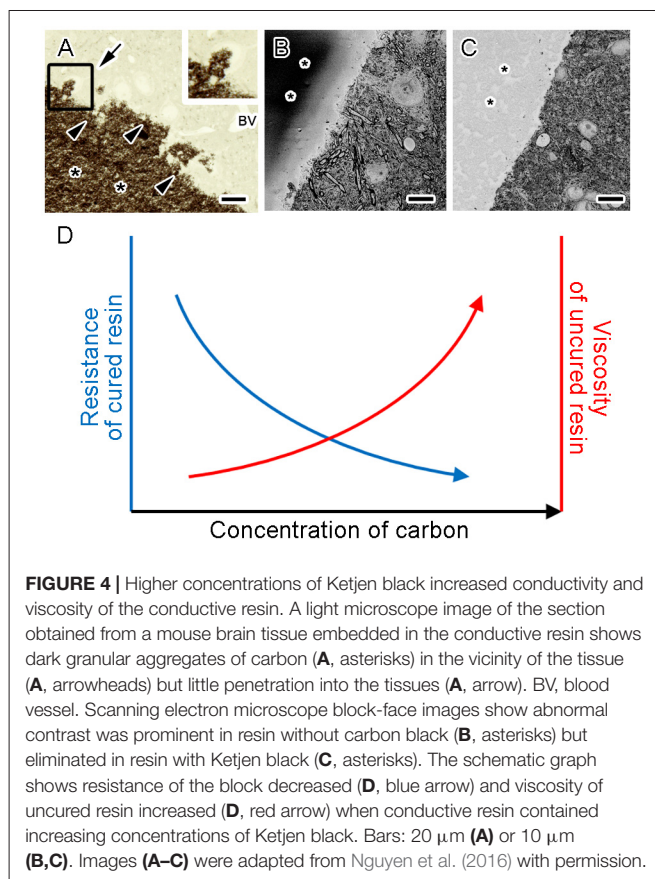
These types of approaches using biological filler materials are promising options to facilitate serial image acquisition using SEM.

Besides biological tissues, other filler materials have been used to modulate the physical properties of resins. For example, the addition of metal particles alters properties such as the electrical and thermal conductivity of plastic (Bhattacharya and Chaklader, 2006). Metallic particles are embedded to image brain tissues by SBEM, where samples with low metal deposition or areas of non-conductive embedding media outside of tissues are susceptible to charging artifacts (**Figure 3B**). Epo-Tek and Epon embedding (EE embedding) uses commercially available epoxy glue containing silver particles, and this technique enables embedding conductive resins with metal particles in the vicinity of target brain samples (Wanner et al., 2016). Although areas with less heavy metal deposition have charging artifacts, this approach facilitated serial imaging of brain samples under high-vacuum conditions. Serial images of 4,750 sections at 25 nm thickness could be acquired in this study, and only one section was lost, proving that EE-embedding is a promising approach and considered to be suitable for ultra-thin sectioning. Recent studies used the same approach, and one of them acquired 11,416 slices of tiled images at 10 nm × 10 nm × 25 nm resolution in SBEM (Genoud et al., 2018; Titze et al., 2018). This approach is further evidence that using conductive metal particles around target samples facilitates serial SEM image acquisition, especially SBEM, which is readily affected by charging artifacts.

Increasing conductivity without influencing the contrast of the embedding medium can be achieved by using conductive materials composed of light elements. Carbon-based materials have relatively high conductivity, and for example, conductive tape covered by carbon nanotubes was used for imaging with ATUM and SEM (Kubota et al., 2018). Carbon black fillers have been used to modify the physical properties of plastics and polymers, such as electrical conductivity and material toughness, and therefore the addition of carbon black to embedding media may improve conductivity without affecting contrast (Yacubowicz et al., 1990; Chekanov et al., 1999; Novák et al., 2005; Domun et al., 2015).

One type of commercially available carbon black, called Ketjen black, reduces the resistance of base resins without altering mechanical stability (Kim et al., 2008). The reduction in resistance depends on the amount of the carbon added to the resin, but Ketjen black increases conductivity at relatively low concentrations (Connor et al., 1998; Chekanov et al., 1999; Balberg, 2002). A more structured carbon black, such as Ketjen black, forms larger agglomerates, which results in networks of conductive fillers with small gaps and improves the conductivity of non-conductive base materials even at lower concentrations (Balberg, 2002). Together, these studies suggest that Ketjen black is the most suitable carbon black for electron microscopy because it efficiently reduces resistance while maintaining mechanical stability.

Indeed, conductive resin produced by Ketjen black is useful for imaging with SBEM under several different sample



preparations (**Figure 3C**; Thai et al., 2016). Ketjen black particles are too large to enter cells and tissues, and therefore cannot penetrate deep inside tissues even when well dispersed in base resins and incubated with samples for a long time (**Figure 4A**). However, the addition of conductive materials in the resin substantially diminishes charging of the samples and resins for SBEM imaging (**Figures 4B,C**; Nguyen et al., 2016). In addition, embedding Ketjen black into resin ameliorates image deformation caused by insufficient sample conductivity, improves slicing quality and facilitates acquisition of serial images at higher resolution (Nguyen et al., 2016). Conductive resins based on carbon black fillers substantially reduce charging artifacts, result in better ultrastructural data and are applicable to various types of tissues in SBEM imaging (Nguyen et al., 2016, 2018; Thai et al., 2016, in press; Yoshimura et al., 2017; Saitoh et al., 2018; Sawada et al., 2018; Takeda et al., 2018).

FUTURE PERSPECTIVES OF THE EMBEDDING MEDIA FOR VOLUME IMAGING

Although the currently available conductive resins have beneficial effects in volume imaging with SEM, there are several drawbacks in their usage. For example, the amount of the carbon black that can be added is limited partly by the increased viscosity of uncured resin (Lee, 1992; Nguyen et al., 2016).

Addition of more Ketjen black into the resin results in further reduction of resistance, and also further increase in viscosity (Figure 4D), which impairs sample embedding. Therefore, the amount of Ketjen black that can be added to the resin is limited by the maximum viscosity acceptable for embedding. It is important to choose the concentration of Ketjen black where the resistance of the cured block and viscosity of the uncured resin are at acceptable levels. This issue might be partly addressed by selection of the base resins with lower viscosity. At the same time, selection of appropriate base resins and embedding media which will reduce deformations from electron irradiation facilitates better serial image acquisition (Kizilyaprak et al., 2015). Future studies might elucidate the optimal selection of the embedding media with acceptable viscosity and deformations, which would significantly facilitate production of conductive resins and acquisition of high quality data from biological specimens.

In addition, carbon-based resins in general require careful dispersion of the carbon powder during mixing with the base resin. Suboptimal dispersion impairs conductivity of the resins produced with the conductive fillers. Metallic filler materials would also have similar requirement of dispersion, and usage of premixed products which are commercially available reduced the burden of manual dispersion of the fillers (Wanner et al., 2016). Development and distribution of such premixed products would be preferred for the future conductive embedding media with conductive filler particles used for electron microscopic imaging.

Lastly, the reduced transparency or complete opacity of the samples applies not only to carbon-filled resins, but also to the other filler materials. These issues are attributable to the non-transparent properties of the filler materials added to the base resins. Although improvement in the conductivity of the base resin could not be achieved so far by addition of transparent and conductive ionic liquid (Nguyen et al., 2016), exploration and application of transparent conductive materials might lead to development of conductive embedding media which is preferred for the identification and orientation of the embedded samples without exposure.

REFERENCES

- Balberg, I. (2002). A comprehensive picture of the electrical phenomena in carbon black-polymer composites. *Carbon* 40, 139–143. doi: 10.1016/s0008-6223(01)00164-6
- Bhattacharya, S. K., and Chaklader, A. C. D. (2006). Review on metal-filled plastics. Part1. Electrical conductivity. *Polym. Plast. Technol. Eng.* 19, 21–51. doi: 10.1080/03602558208067726
- Bock, D. D., Lee, W.-C., Kerlin, A. M., Andermann, M. L., Hood, G., Wetzell, A. W., et al. (2011). Network anatomy and *in vivo* physiology of visual cortical neurons. *Nature* 471, 177–182. doi: 10.1038/nature09802
- Briggman, K. L., and Bock, D. D. (2012). Volume electron microscopy for neuronal circuit reconstruction. *Curr. Opin. Neurobiol.* 22, 154–161. doi: 10.1016/j.conb.2011.10.022
- Briggman, K. L., Helmstaedter, M., and Denk, W. (2011). Wiring specificity in the direction-selectivity circuit of the retina. *Nature* 471, 183–188. doi: 10.1038/nature09818
- Brightman, M. W., and Reese, T. S. (1969). Junctions between intimately apposed cell membranes in the vertebrate brain. *J. Cell Biol.* 40, 648–677. doi: 10.1083/jcb.40.3.648

CONCLUDING REMARKS

During the past several years, there have been rapid methodological advancements for volume imaging of large biological specimens with SEM including increased options for staining, embedding and observation. Conductive materials are a unique option for better quality of images by reducing the charging of sample blocks in serial image acquisition with SEM, which is prone to charging artifacts. The available methods still have many limitations, and future studies involving the development and application of novel materials and a combination of available modifications may lead to better scale, quality, and throughput for the three-dimensional ultrastructural analyses of biological samples. These efforts will enable a deeper understanding of neural circuitry and provide the structural foundation for basic and higher brain functions.

AUTHOR CONTRIBUTIONS

All authors contributed to the writing and approved the final version of the manuscript.

FUNDING

This work is partly supported by Japan Society for the Promotion of Science (JSPS) KAKENHI Grant Number 16K12345 (to NO), Research Grant from National Center of Neurology and Psychiatry (No. 30-5 to NO), Cooperative Research Program of “Network Joint Research Center for Materials and Devices” and Cooperative Study Programs of National Institute for Physiological Sciences (to NO).

ACKNOWLEDGMENTS

We thank Dr. Toshiyuki Oda in University of Yamanashi for providing some images. We would like to thank Setsuro Fujii Memorial, Osaka Foundation for Promotion of Fundamental Medical Research, for providing the support.

- Chekanov, Y., Ohnogi, R., Asai, S., and Sumita, M. (1999). Electrical properties of epoxy resin filled with carbon fibers. *J. Mater. Sci.* 34, 5589–5592. doi: 10.1023/A:1004737217503
- Connor, M. T., Roy, S., Ezquerro, T. A., and Baltá Calleja, F. J. (1998). Broadband ac conductivity of conductor-polymer composites. *Phys. Rev. B* 57, 2286–2294. doi: 10.1103/physrevb.57.2286
- Deco, G., and Kringelbach, M. L. (2014). Great expectations: using whole-brain computational connectomics for understanding neuropsychiatric disorders. *Neuron* 84, 892–905. doi: 10.1016/j.neuron.2014.08.034
- Deerinck, T. J., Bushong, E. A., Lev-Ram, V., Shu, X., Tsien, R. Y., and Ellisman, M. H. (2010). Enhancing serial block-face scanning electron microscopy to enable high resolution 3-D nanohistology of cells and tissues. *Microsc. Microanal.* 16, 1138–1139. doi: 10.1017/s1431927610055170
- Deerinck, T. J., Shone, T. M., Bushong, E. A., Ramachandra, R., Peltier, S. T., and Ellisman, M. H. (2017). High-performance serial block-face SEM of nonconductive biological samples enabled by focal gas injection-based charge compensation. *J. Microsc.* 270, 142–149. doi: 10.1111/jmi.12667
- Denk, W., and Horstmann, H. (2004). Serial block-face scanning electron microscopy to reconstruct three-dimensional tissue nanostructure. *PLoS Biol.* 2:e329. doi: 10.1371/journal.pbio.0020232

- Domun, N., Hadavinia, H., Zhang, T., Sainsbury, T., Liaghat, G. H., and Vahid, S. (2015). Improving the fracture toughness and the strength of epoxy using nanomaterials—a review of the current status. *Nanoscale* 7, 10294–10329. doi: 10.1039/c5nr01354b
- Eberle, A. L., Selchow, O., Thaler, M., Zeidler, D., and Kirmse, R. (2015). Mission (im)possible—mapping the brain becomes a reality. *Microscopy* 64, 45–55. doi: 10.1093/jmicro/dfu104
- Fenno, L., Yizhar, O., and Deisseroth, K. (2011). The development and application of optogenetics. *Annu. Rev. Neurosci.* 34, 389–412. doi: 10.1146/annurev-neuro-061010-113817
- Filippi, M., van den Heuvel, M. P., Fornito, A., He, Y., Hulshoff Pol, H. E., Agosta, F., et al. (2013). Assessment of system dysfunction in the brain through MRI-based connectomics. *Lancet Neurol.* 12, 1189–1199. doi: 10.1016/s1474-4422(13)70144-3
- Fornito, A., Zalesky, A., and Breakspear, M. (2015). The connectomics of brain disorders. *Nat. Rev. Neurosci.* 16, 159–172. doi: 10.1038/nrn3901
- Genoud, C., Titzte, B., Graff-Meyer, A., and Friedrich, R. W. (2018). Fast homogeneous *En Bloc* staining of large tissue samples for volume electron microscopy. *Front. Neuroanat.* 12:76. doi: 10.3389/fnana.2018.00076
- Glauert, A. M., and Glauert, R. H. (1958). Araldite as an embedding medium for electron microscopy. *J. Biophys. Biochem. Cytol.* 4, 191–194. doi: 10.1083/jcb.4.2.191
- Gong, S., Zheng, C., Doughty, M. L., Losos, K., Didkovsky, N., Schambra, U. B., et al. (2003). A gene expression atlas of the central nervous system based on bacterial artificial chromosomes. *Nature* 425, 917–925. doi: 10.1038/nature02033
- Grienberger, C., and Konnerth, A. (2012). Imaging calcium in neurons. *Neuron* 73, 862–885. doi: 10.1016/j.neuron.2012.02.011
- Hall, D. H., Hartwig, E., and Nguyen, K. C. (2012). Modern electron microscopy methods for *C. elegans*. *Methods Cell Biol.* 107, 93–149. doi: 10.1016/B978-0-12-394620-1.00004-7
- Harris, K. M., Perry, E., Bourne, J., Feinberg, M., Ostroff, L., and Hurlburt, J. (2006). Uniform serial sectioning for transmission electron microscopy. *J. Neurosci.* 26, 12101–12103. doi: 10.1523/JNEUROSCI.3994-06.2006
- Hashimoto, T., Thompson, G. E., Zhou, X., and Withers, P. J. (2016). 3D imaging by serial block face scanning electron microscopy for materials science using ultramicrotomy. *Ultramicroscopy* 163, 6–18. doi: 10.1016/j.ultramicro.2016.01.005
- Hayworth, K. J., Morgan, J. L., Schalek, R., Berger, D. R., Hildebrand, D. G., and Lichtman, J. W. (2014). Imaging ATUM ultrathin section libraries with WaferMapper: a multi-scale approach to EM reconstruction of neural circuits. *Front. Neural Circuits* 8:68. doi: 10.3389/fncir.2014.00068
- Hennig, P., and Denk, W. (2007). Point-spread functions for backscattered imaging in the scanning electron microscope. *J. Appl. Phys.* 102:123101. doi: 10.1063/1.2817591
- Hildebrand, D. G. C., Cicconet, M., Torres, R. M., Choi, W., Quan, T. M., Moon, J., et al. (2017). Whole-brain serial-section electron microscopy in larval zebrafish. *Nature* 545, 345–349. doi: 10.1038/nature22356
- Holcomb, P. S., Hoffpauir, B. K., Hoyson, M. C., Jackson, D. R., Deerinck, T. J., Marrs, G. S., et al. (2013). Synaptic inputs compete during rapid formation of the calyx of Held: a new model system for neural development. *J. Neurosci.* 33, 12954–12969. doi: 10.1523/JNEUROSCI.1087-13.2013
- Hua, Y., Laserstein, P., and Helmstaedter, M. (2015). Large-volume en-bloc staining for electron microscopy-based connectomics. *Nat. Commun.* 6:7923. doi: 10.1038/ncomms8923
- Hukui, I. (1996). Tissue preparation for reconstruction of large-scale three-dimensional structures using a scanning electron microscope. *J. Microsc.* 182, 95–101. doi: 10.1111/j.1365-2818.1996.tb04796.x
- Ichimura, K., Miyazaki, N., Sadayama, S., Murata, K., Koike, M., Nakamura, K., et al. (2015). Three-dimensional architecture of podocytes revealed by block-face scanning electron microscopy. *Sci. Rep.* 5:8993. doi: 10.1038/srep08993
- Karnovsky, M. J. (1971). “Use of ferrocyanide-reduced osmium tetroxide in electron microscopy,” in *Abstracts of the American Society for Cell Biology* (New Orleans, LA), p.146.
- Kasthuri, N., Hayworth, K. J., Berger, D. R., Schalek, R. L., Conchello, J. A., Knowles-Barley, S., et al. (2015). Saturated reconstruction of a volume of neocortex. *Cell* 162, 648–661. doi: 10.1016/j.cell.2015.06.054
- Katoh, M., Wu, B., Nguyen, H. B., Thai, T. Q., Yamasaki, R., Lu, H., et al. (2017). Polymorphic regulation of mitochondrial fission and fusion modifies phenotypes of microglia in neuroinflammation. *Sci. Rep.* 7:4942. doi: 10.1038/s41598-017-05232-0
- Kim, B. C., Park, S. W., and Lee, D. G. (2008). Fracture toughness of the nano-particle reinforced epoxy composite. *Compos. Struct.* 86, 69–77. doi: 10.1016/j.compstruct.2008.03.005
- Kizilyaprak, C., Longo, G., Daraspe, J., and Humbel, B. M. (2015). Investigation of resins suitable for the preparation of biological sample for 3-D electron microscopy. *J. Struct. Biol.* 189, 135–146. doi: 10.1016/j.jsb.2014.10.009
- Knott, G., Marchman, H., Wall, D., and Lich, B. (2008). Serial section scanning electron microscopy of adult brain tissue using focused ion beam milling. *J. Neurosci.* 28, 2959–2964. doi: 10.1523/JNEUROSCI.3189-07.2008
- Kubota, Y., Karube, F., Nomura, M., Gullledge, A. T., Mochizuki, A., Schertel, A., et al. (2011). Conserved properties of dendritic trees in four cortical interneuron subtypes. *Sci. Rep.* 1:89. doi: 10.1038/srep00089
- Kubota, Y., Sohn, J., Hatada, S., Schurr, M., Straehle, J., Gour, A., et al. (2018). A carbon nanotube tape for serial-section electron microscopy of brain ultrastructure. *Nat. Commun.* 9:437. doi: 10.1038/s41467-017-02768-7
- Le Bihan, D., Mangin, J. F., Poupon, C., Clark, C. A., Pappata, S., Molko, N., et al. (2001). Diffusion tensor imaging: concepts and applications. *J. Magn. Reson. Imaging* 13, 534–546. doi: 10.1002/jmri.1076
- Leduc, E. H., and Bernhard, W. (1967). Recent modifications of the glycol methacrylate embedding procedure. *J. Ultrastruct. Res.* 19, 196–199. doi: 10.1016/s0022-5320(67)80068-6
- Lee, B. L. (1992). Electrically conductive polymer composites and blends. *Polym. Eng. Sci.* 32, 36–42. doi: 10.1002/pen.760320107
- Lichtman, J. W., Pfister, H., and Shavit, N. (2014). The big data challenges of connectomics. *Nat. Neurosci.* 17, 1448–1454. doi: 10.1038/nn.3837
- Livet, J., Weissman, T. A., Kang, H., Draft, R. W., Lu, J., Bennis, R. A., et al. (2007). Transgenic strategies for combinatorial expression of fluorescent proteins in the nervous system. *Nature* 450, 56–62. doi: 10.1038/nature06293
- Luft, J. H. (1961). Improvements in epoxy resin embedding methods. *J. Biophys. Biochem. Cytol.* 9, 409–414. doi: 10.1083/jcb.9.2.409
- Luther, P. K. (2006). “Sample shrinkage and radiation damage of plastic sections,” in *Electron Tomography Methods for Three-Dimensional Visualization of Structures in the Cell*, ed. J. Frank (New York, NY: Springer), 17–48.
- Mathieu, C. (1999). The beam-gas and signal-gas interactions in the variable pressure scanning electron microscope. *Scanning Microsc.* 13, 23–41.
- Mikula, S., and Denk, W. (2015). High-resolution whole-brain staining for electron microscopic circuit reconstruction. *Nat. Methods* 12, 541–546. doi: 10.1038/nmeth.3361
- Morgan, J. L., Berger, D. R., Wetzel, A. W., and Lichtman, J. W. (2016). The fuzzy logic of network connectivity in mouse visual thalamus. *Cell* 165, 192–206. doi: 10.1016/j.cell.2016.02.033
- Möller-Reichert, T., Hohenberg, H., O’Toole, E. T., and McDonald, K. (2003). Cryoimmobilization and three-dimensional visualization of *C. elegans* ultrastructure. *J. Microsc.* 212, 71–80. doi: 10.1046/j.1365-2818.2003.01250.x
- Nguyen, H. B., Sui, Y., Thai, T. Q., Ikenaka, K., Oda, T., and Ohno, N. (2018). Decreased number and increased volume with mitochondrial enlargement of cerebellar synaptic terminals in a mouse model of chronic demyelination. *Med. Mol. Morphol.* 51, 208–216. doi: 10.1007/s00795-018-0193-z
- Nguyen, H. B., Thai, T. Q., Saitoh, S., Wu, B., Saitoh, Y., Shimo, S., et al. (2016). Conductive resins improve charging and resolution of acquired images in electron microscopic volume imaging. *Sci. Rep.* 6:23721. doi: 10.1038/srep23721
- Novák, I., Krupa, I., and Janigová, I. (2005). Hybrid electro-conductive composites with improved toughness, filled by carbon black. *Carbon* 43, 841–848. doi: 10.1016/j.carbon.2004.11.019
- Ohno, N., Chiang, H., Mahad, D. J., Kidd, G. J., Liu, L., Ransohoff, R. M., et al. (2014). Mitochondrial immobilization mediated by syntaphilin facilitates survival of demyelinated axons. *Proc. Natl. Acad. Sci. U S A* 111, 9953–9958. doi: 10.1073/pnas.1401155111
- Ohno, N., Katoh, M., Saitoh, Y., and Saitoh, S. (2016). Recent advancement in the challenges to connectomics. *Microscopy* 65, 97–107. doi: 10.1093/jmicro/dfv371
- Ohno, N., Katoh, M., Saitoh, Y., Saitoh, S., and Ohno, S. (2015). Three-dimensional volume imaging with electron microscopy toward connectome. *Microscopy* 64, 17–26. doi: 10.1093/jmicro/dfu112

- Ohta, K., Sadayama, S., Togo, A., Higashi, R., Tanoue, R., and Nakamura, K. (2012). Beam deceleration for block-face scanning electron microscopy of embedded biological tissue. *Micron* 43, 612–620. doi: 10.1016/j.micron.2011.11.001
- Osten, P., and Margrie, T. W. (2013). Mapping brain circuitry with a light microscope. *Nat. Methods* 10, 515–523. doi: 10.1038/nmeth.2477
- Palay, S. L. (1958). The morphology of synapses in the central nervous system. *Exp. Cell Res.* 14, 275–293.
- Richards, R. G., and Gwynn, I. A. (1995). Backscattered electron imaging of the undersurface of resin-embedded cells by field-emission scanning electron microscopy. *J. Microsc.* 177, 43–52. doi: 10.1111/j.1365-2818.1995.tb03532.x
- Saitoh, S., Ohno, N., Saitoh, Y., Terada, N., Shimo, S., Aida, K., et al. (2018). Improved serial sectioning techniques for correlative light-electron microscopy mapping of human langerhans islets. *Acta Histochem. Cytochem.* 51, 9–20. doi: 10.1267/ahc.17020
- Sawada, M., Ohno, N., Kawaguchi, M., Huang, S. H., Hikita, T., Sakurai, Y., et al. (2018). PlexinD1 signaling controls morphological changes and migration termination in newborn neurons. *EMBO J.* 37:e97404. doi: 10.15252/embj.201797404
- Seligman, A. M., Wasserkrug, H. L., and Hanker, J. S. (1966). A new staining method (OTO) for enhancing contrast of lipid-containing membranes and droplets in osmium tetroxide—fixed tissue with osmiophilic thiocarbonylhydrazide(TCH). *J. Cell Biol.* 30, 424–432. doi: 10.1083/jcb.30.2.424
- Staubli, W. (1963). A new embedding technique for electron microscopy, combining a water-soluble epoxy resin (Durcupan) with water-insoluble Araldite. *J. Cell Biol.* 16, 197–201. doi: 10.1083/jcb.16.1.197
- Takeda, A., Shinozaki, Y., Kashiwagi, K., Ohno, N., Eto, K., Wake, H., et al. (2018). Microglia mediate non-cell-autonomous cell death of retinal ganglion cells. *Glia* doi: 10.1002/glia.23475 [Epub ahead of print].
- Tapia, J. C., Kasthuri, N., Hayworth, K. J., Schalek, R., Lichtman, J. W., Smith, S. J., et al. (2012). High-contrast en bloc staining of neuronal tissue for field emission scanning electron microscopy. *Nat. Protoc.* 7, 193–206. doi: 10.1038/nprot.2011.439
- Terasaki, M., Shemesh, T., Kasthuri, N., Klemm, R. W., Schalek, R., Hayworth, K. J., et al. (2013). Stacked endoplasmic reticulum sheets are connected by helicoidal membrane motifs. *Cell* 154, 285–296. doi: 10.1016/j.cell.2013.06.031
- Thai, T. Q., Nguyen, H. B., Saitoh, S., Wu, B., Saitoh, Y., Shimo, S., et al. (2016). Rapid specimen preparation to improve the throughput of electron microscopic volume imaging for three-dimensional analyses of subcellular ultrastructures with serial block-face scanning electron microscopy. *Med. Mol. Morphol.* 49, 154–162. doi: 10.1007/s00795-016-0134-7
- Thai, T. Q., Nguyen, H. B., Sui, Y., Ikenaka, K., Oda, T., and Ohno, N. (in press). Interactions between mitochondria and endoplasmic reticulum in demyelinated axons. *Med. Mol. Morphol.*
- Thiel, B., Bache, I., Fletcher, A., Meredith, P., and Donald, A. (1997). An improved model for gaseous amplification in the environmental SEM. *J. Microsc.* 187, 143–157. doi: 10.1046/j.1365-2818.1997.2360794.x
- Titze, B., and Denk, W. (2013). Automated in-chamber specimen coating for serial block-face electron microscopy. *J. Microsc.* 250, 101–110. doi: 10.1111/jmi.12023
- Titze, B., Genoud, C., and Friedrich, R. W. (2018). SBEMImage: versatile acquisition control software for serial block-face electron microscopy. *Front. Neural Circuits* 12:54. doi: 10.3389/fncir.2018.00054
- Walton, J. (1979). Lead aspartate, an en bloc contrast stain particularly useful for ultrastructural enzymology. *J. Histochem. Cytochem.* 27, 1337–1342. doi: 10.1177/27.10.512319
- Wanner, A. A., Genoud, C., Masudi, T., Siksou, L., and Friedrich, R. W. (2016). Dense EM-based reconstruction of the interglomerular projectome in the zebrafish olfactory bulb. *Nat. Neurosci.* 19, 816–825. doi: 10.1038/nn.4290
- Wergin, W. P., Yaklich, R. W., Roy, S., Joy, D. C., Erbe, E. F., Murphy, C. A., et al. (1997). Imaging thin and thick sections of biological tissue with the secondary electron detector in a field-emission scanning electron microscope. *Scanning* 19, 386–395. doi: 10.1002/sca.4950190601
- Wilt, B. A., Burns, L. D., Wei Ho, E. T., Ghosh, K. K., Mukamel, E. A., and Schnitzer, M. J. (2009). Advances in light microscopy for neuroscience. *Annu. Rev. Neurosci.* 32, 435–506. doi: 10.1146/annurev.neuro.051508.135540
- Yacobowicz, J., Narkis, M., and Benguigui, L. (1990). Electrical and dielectric properties of segregated carbon black-polyethylene systems. *Polym. Eng. Sci.* 30, 459–468. doi: 10.1002/pen.760300806
- Yin, X., Kidd, G. J., Ohno, N., Perkins, G. A., Ellisman, M. H., Bastian, C., et al. (2016). Proteolipid protein-deficient myelin promotes axonal mitochondrial dysfunction via altered metabolic coupling. *J. Cell Biol.* 215, 531–542. doi: 10.1083/jcb.201607099
- Yoshimura, T., Hayashi, A., Handa-Narumi, M., Yagi, H., Ohno, N., Koike, T., et al. (2017). GlcNAc6ST-1 regulates sulfation of N-glycans and myelination in the peripheral nervous system. *Sci. Rep.* 7:42257. doi: 10.1038/srep42257

Conflict of Interest Statement: The authors declare that the research was conducted in the absence of any commercial or financial relationships that could be construed as a potential conflict of interest.

The handling editor declared a shared affiliation, though no other collaboration, with several of the authors HN, TT and NO at time of review.

Copyright © 2018 Nguyen, Thai, Sui, Azuma, Fujiwara and Ohno. This is an open-access article distributed under the terms of the Creative Commons Attribution License (CC BY). The use, distribution or reproduction in other forums is permitted, provided the original author(s) and the copyright owner(s) are credited and that the original publication in this journal is cited, in accordance with accepted academic practice. No use, distribution or reproduction is permitted which does not comply with these terms.